# Vibrational Sum-Frequency Studies of a Series of Phospholipid Monolayers and the Associated Water Structure at the Vapor/Water Interface

**Mark R. Watry, Teresa L. Tarbuck, and Geraldine L. Richmond***

*Department of Chemistry, University of Oregon, Eugene, Oregon 97403*

*Received: July 22, 2002*

The orientation and conformation of phospholipid monolayers and the structure of water associated with these monolayers adsorbed at the vapor/water interface have been investigated using vibrational sum-frequency spectroscopy. The phospholipids studied are saturated diacyl phosphatidylcholines, phosphatidylethanolamines, phosphatidylglycerols, and phosphatidylserines with chain lengths of 14, 16, and 18 carbons. Spectra have been acquired under different polarization schemes for monolayers at the vapor/$D_2O$ interface to examine chain ordering and at the vapor/$H_2O$ interface to examine water structure. Comparisons are made between the monolayers based on chain length and headgroup differences. These studies show significant differences between the aqueous environments associated with the zwitterionic lipids and the charged lipids.

## Introduction

Biomembranes are assembled from a diverse group of molecules including lipids, sterols, and proteins, and each subgroup is quite diverse in itself. Among the many types of lipids residing in biomembranes, phospholipids constitute the major component of most cell membranes and play an important role in the functioning of the membrane. At physiologically relevant neutral pH, some phospholipids such as phosphatidylcholine and phosphatidylethanolamine carry no net charge but are zwitterionic, whereas others such as phosphatidylglycerol and phosphatidylserine carry a net negative charge. The molecules in a biomembrane assemble into a bilayer structure with a nonsymmetric distribution of charge, i.e., one lipid layer of the bilayer or the other tends to contain the majority of the charged species.[1] In other cases, the charged lipids may form domains.[2,3]

The highly complex and inhomogeneous composition of natural membranes necessitates the study of simpler, although still quite complex, model membranes. Phospholipid monolayers provide simplified model systems of biomembranes,[4] and given the physiological importance of the phospholipids themselves, phospholipid monolayers have been the subject of intense scientific inquiry for over 30 years.[5−7] The most widely studied phospholipids are the phosphatidylcholines[8,9] due to their widespread inclusion in cell membranes as a structural component. The study of phospholipid monolayers is also relevant to understanding the behavior of lung surfactant, of which dipalmitoylphosphatidylcholine is the major component.[10] The phosphocholines, however, coexist with other phospholipids in real biological systems. Each has its effect on the properties of the membrane, yet none are so radically different that the membrane falls apart. Examination of acyl chain ordering can be used to elucidate these differences since chain−chain interactions determine the fluidity of membranes.

Natural biological membranes are designed to enclose aqueous solution and are usually found in an aqueous environment. The interaction between the water molecules and the membrane affects the structure of both the membrane and of the water associated with the membrane.[11] An understanding of the water structure in individual phospholipid monolayers can be utilized to determine the effects of headgroup composition on membrane structure.

In this paper, we employ an interfacially specific nonlinear vibrational spectroscopy to examine the orientation and conformation of phospholipid molecules in monolayers and the hydrogen-bonding network of water molecules associated with the monolayer at the vapor/monolayer/water interface. The ordering of the acyl chains as a function of chain length and headgroup identity in various phospholipid monolayers at the vapor/water interface is investigated as well as the effect of the different phospholipid headgroups on the structure of the water molecules at this interface. The phospholipids employed in this study are saturated diacyl phosphatidylcholines, phosphatidylethanolamines, phosphatidylglycerols, and phosphatidylserines with chain lengths of 14, 16, and 18 carbons (see Figure 1).

## Background

**Sum Frequency and Analysis.** VSFS was first treated theoretically by Bloembergen and Pershan in 1962[12] and was first demonstrated experimentally by the Shen laboratory in 1987.[13,14] It is a second-order nonlinear optical technique that provides vibrational spectra of molecules present at the interface between two centrosymmetric media. In the experiment, a laser beam with a fixed visible frequency and a tunable infrared beam are overlapped spatially and temporally at the interface. These beams induce a nonlinear polarization in the media that generates a coherent beam at the sum of the two incident frequencies.[12,15−19] The sum-frequency intensity depends on the square of the second-order polarization and, in turn, the square of the nonlinear susceptibility and the incident electric fields:

$$I(\omega_{sfg}) \propto |P^{(2)}|^2 \propto |\chi^{(2)}:\ E_{vis}E_{IR}|^2 \qquad (1)$$

where $\chi^{(2)}$ is the macroscopic second-order susceptibility of the medium. The sum-frequency conversion efficiency is enhanced when the infrared beam is on resonance with a molecular

* Author to whom correspondence should be addressed.

10.1021/jp0216878 CCC: $25.00 
Published on Web 12/18/2002

vibration. The resonant contributions to the nonlinear susceptibility are separable from the nonresonant contribution:

$$\chi^{(2)} = \chi^{(2)}_{NR} + \sum_{v} \chi^{(2)}_{R}(v) \qquad (2)$$

where the sum is over all vibrational modes of all molecular species in the medium. In general, the nonresonant response is small for liquid surfaces;[15] however, it is not negligible at the vapor/water interface.[20] The resonant sum-frequency response is a sum of resonant peaks that can be described by the second term in the following equation for the total second-order susceptibility:

$$\chi^{(2)} = \chi^{(2)}_{NR}\, e^{i\phi} + \sum_{v} \int_{-\infty}^{\infty} \frac{A_v e^{i\phi_v} e^{-[\omega_L - \omega_v/\Gamma_v]^2}}{\omega_{IR} - \omega_L + i\Gamma_L}\, d\omega_L \qquad (3)$$

This form of the resonant response for a vibration was first used by Bain[16] and convolves the homogeneous line width of the transition (HWHM, $\Gamma_L$) with inhomogeneous broadening (FWHM, $\sqrt{2\ln 2}\,\Gamma_v$) from the multitude of molecular environments present in the condensed phase. $A_v$, a complex quantity, is proportional to the product of the number of molecules probed and their orientationally averaged IR and Raman transition probabilities. It can be thought of as the sum-frequency transition strength.

## Experimental

**Laser System.** The laser system used in these studies has been thoroughly described previously[21,22] so only a brief summary will be given here. The amplified output of a Ti:Sapphire system produces 2 ps pulses of 800 nm light at a 1 kHz repetition rate. Approximately 200 $\mu$J of energy is directed to the interface as the visible pulse, and the remainder is utilized in an OPG stage and two OPA stages to produce 4−13 $\mu$J of tunable IR from 2700 to 4000 cm$^{-1}$. The beams are combined at the interface in a co-propagating geometry with the visible beam striking the interface at 56° from the surface normal and the IR beam at 67° to the surface normal. The reflected sum-frequency beam is collected with a thermoelectrically cooled CCD camera with data recorded by tuning the IR in 0.0025 $\mu$m steps and taking a timed exposure at each step. Spectra were acquired under *ssp* and *sps* polarization schemes (SF, Vis, IR) where *p*-polarized light is polarized in the plane of incidence and *s*-polarized light is polarized normal to the plane of incidence.

Interaction between the tunable IR beam and water vapor in the air results in considerable temporal lengthening of the 2 ps pulses between 3600 and 3800 cm$^{-1}$. To correct for this temporal dephasing and the frequency dependence of the IR energy, each SF spectrum has been divided by the nonresonant sum-frequency response from gold which would have a constant intensity in the absence of water vapor and variations in the IR energy as a function of wavelength. Simultaneously, any wavelength-dependent effects introduced into the sum-frequency signal by the collection optics are corrected.

**Sample Preparation.** Lipids were purchased as lyophilized powders from Avanti Polar Lipids, chloroform (99+% A.C.S. HPLC grade) from Aldrich, anhydrous methyl alcohol from Mallinckrodt, $D_2O$ (d99.9%) from Cambridge Isotopes. Each was used as received. Sodium phosphate monobasic and sodium phosphate dibasic were purchased from Mallinckrodt and dried before use in preparing buffers. Stock spreading solutions of each lipid were prepared by dissolving a few milligrams of lipid in chloroform:methanol (24:1 by volume) so that ~50 $\mu$L of solution was sufficient to prepare a complete monolayer on 10 mM phosphate buffered $D_2O$ or Nanopure water (17.8 MΩ resistivity). Spectroscopic samples were prepared in custom glass dishes ~3.7 cm in diameter by pipetting 9 mL of the appropriate aqueous solution into the dish followed by spreading the lipid using a 50 $\mu$L syringe. All glassware that came in contact with any solution was cleaned in NoChromix Reagent and rinsed with copious amounts of Nanopure water. The syringe was rinsed several times with spreading solvent before and after spreading a monolayer to prevent cross contamination between stock solutions. Stock solutions were used for a maximum of 2 days and were stored in a refrigerator between uses.

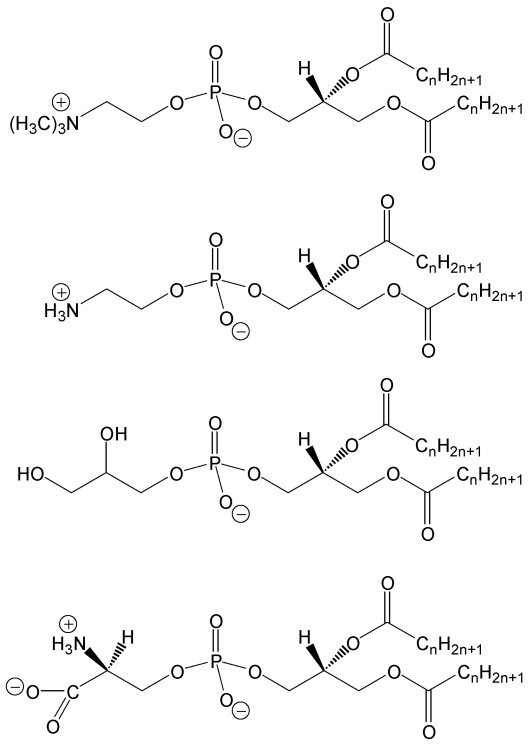


**Figure 1.** Phospholipid structures from top to bottom, respectively: phosphatidylcholine (PC), phosphatidylethanolamine (PE), phosphatidylglycerol (PG), and phosphatidylserine (PS). Chain lengths are denoted by the prefixes: DM for dimyristoyl ($C_{14}$), DP for dipalmitoyl ($C_{16}$), and DS for distearoyl ($C_{18}$).

## Results and Discussion

**Chain Order.** Previous work in this laboratory examining compact phosphatidylcholine monolayers at the $CCl_4/D_2O$ interface showed that there is a transition from disordered acyl chains to well-ordered acyl chains when chain length increases from 16 carbons (or fewer) to 18 carbons or more.[23] Phospholipids with acyl chains of these lengths are the most common in cell membranes and likely affect the fluidity/rigidity of the membrane.

Figures 2a−d show VSFS spectra of monolayers of phosphatidylcholine, phosphatidylethanolamine, phosphatidylglycerol, and phosphatidylserine, respectively, at the vapor/$D_2O$ interface on pH 7.0 buffer (10 mM phosphate). $D_2O$ is used in place of $H_2O$ to allow collection of the C−H stretching spectrum of the phospholipids with minimal interference from water stretching modes. Three spectra are presented for each headgroup, corresponding to saturated diacyl chains of 14, 16, and 18 carbons. The spectra cover the C−H stretching region under *ssp* polarization. The IR and Raman spectral features of alkyl

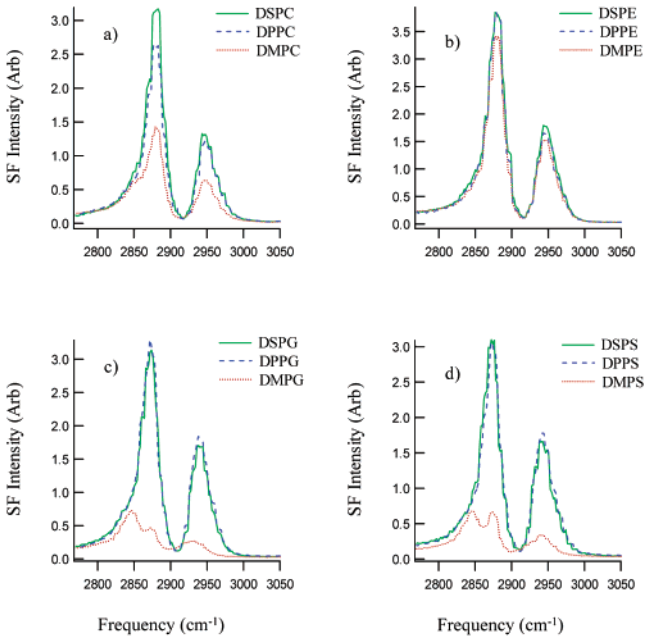


**Figure 2.** Sum-frequency spectra of phospholipid monolayers in the C−H stretching region at the vapor/$D_2O$ interface (10 mM phosphate buffer pD 7.0) acquired under *ssp* polarization. (a) Phosphatidylcholines (b) phosphatidylethanolamines, (c) phosphatidylglycerols, (d) phosphatidylserines.

**TABLE 1: Vibrational Assignments for VSFS Peaks in the C−H Stretching Region (2800−3000 cm$^{-1}$) from Spectral Fits to *ssp* and *sps* Data at the Vapor/$D_2O$ Interface (Uncertainties are within 5 cm$^{-1}$)**

| lipid | $CH_2SS$ | $CH_3SS$ | $CH_2FR$ | $CH_3FR$ | $CH_3AS$ |
|---|---|---|---|---|---|
| DMPC | 2855 | 2883 | 2897 | 2946 | 2962 |
| DPPC | 2854 | 2883 | 2897 | 2946 | 2959 |
| DSPC | 2854 | 2883 | 2897 | 2946 | 2959 |
| DMPE | 2855 | 2883 | 2897 | 2944 | 2958 |
| DPPE | 2855 | 2883 | 2897 | 2944 | 2958 |
| DSPE | 2855 | 2883 | 2897 | 2944 | 2958 |
| DMPG | 2851 | 2879 | 2900 | 2940 | 2958 |
| DPPG | 2847 | 2879 | 2893 | 2940 | 2957 |
| DSPG | 2847 | 2879 | 2893 | 2940 | 2957 |
| DMPS | 2852 | 2879 | 2898 | 2934 | 2958 |
| DPPS | 2851 | 2877 | 2897 | 2938 | 2957 |
| DSPS | 2851 | 2877 | 2896 | 2938 | 2957 |

chains in the C−H stretching region of these phospholipids have been previously assigned.[24−26] Similar assignments have been made for the acyl chains of phospholipids in previous VSF studies.[27,28] The same general assignments are used here with peak positions determined for these studies from fits to the data employing eq 3.

The spectra from each of the monolayers exhibit similar peak positions for all headgroups and chain lengths. The spectra also exhibit similar intensities for each chain length regardless of headgroup identity except for DMPE. The assignments for each monolayer as determined from the fits are given in Table 1 and have uncertainties of one or two wavenumbers. The peak at ~2850 cm$^{-1}$ is assigned to the methylene symmetric stretch ($CH_2SS$), the peak at ~2880 cm$^{-1}$ to the methyl symmetric stretch ($CH_3SS$), and the broad peak at ~2897 cm$^{-1}$ to the methylene Fermi resonance ($CH_2FR$). The peak at ~2940 cm$^{-1}$ is assigned to the methyl Fermi resonance ($CH_3FR$) with the possibility of some contribution from methylene asymmetric stretch ($CH_2AS$). Both the $CH_3FR$ and $CH_2AS$ have been assigned to peaks in this region in previous VSF studies.[16,27−31]

When applying the fitting routine to the *ssp* data, several parameters were constrained. Since it is not possible to separate the natural line widths of the transitions $\Gamma_L$ from the inhomogeneous broadening $\Gamma_\nu$ in these experiments, $\Gamma_L$ was set at 2 cm$^{-1}$ and only $\Gamma_\nu$ was allowed to vary.[29] The methylene modes, $CH_2SS$ and $CH_2FR$, are in phase due to symmetry considerations and are given the relative phase of zero. In addition, the relative phase difference between the $CH_3SS$ and the $CH_3AS$ is $\pi$ due to symmetry,[32,33] and the $CH_3FR$ is in phase with the methyl symmetric stretch, also due to symmetry. A nonresonant contribution to the susceptibility is included in the fits to account for intensity above 3000 cm$^{-1}$. The nonresonant contribution is independent of wavelength and enters the fit having a constant amplitude and phase. The spectra were fit as a consistent set using the same vibrational peaks and relative phases in every fit.

**TABLE 2: Ratio of the Square Root of the Methyl Symmetric Stretch Intensity to the Square Root of the Methylene Symmetric Stretch Intensity from the *ssp* Spectra for Each Phospholipid Monolayer**

| lipid | ratio | lipid | ratio |
|---|---|---|---|
| DMPC | 2.5 ± 0.5 | DMPG | 0.5 ± 0.2 |
| DPPC | 4.7 ± 1.1 | DPPG | 4.5 ± 1.1 |
| DSPC | 7.9 ± 1.3 | DSPG | 4.4 ± 1.1 |
| DMPE | 4.9 ± 1.2 | DMPS | 1.1 ± 0.3 |
| DPPE | 6.4 ± 1.3 | DPPS | 5.5 ± 1.2 |
| DSPE | 5.3 ± 1.2 | DSPS | 5.0 ± 1.2 |

A useful parameter for examining the relative ordering of alkyl chains in linear spectroscopy is the ratio of the integrated methyl symmetric stretch intensity to the integrated methylene symmetric stretch intensity.[24] In VSFS a ratio of the square root of the integrated areas of these two peaks is employed since these values are proportional to the number of molecules contributing to the SF intensity. If the incoming IR beam is *p*-polarized, the IR transition moment for the methyl symmetric stretch in an all-trans chain is aligned with the IR electric field resulting in a large SF signal. However, since there are local inversion centers at the center of each C−C bond in an all-trans chain, intensity in the methylene symmetric stretch is forbidden under the dipole approximation. Conversely, under this same polarization (*ssp*), highly disordered chains lead to a more isotropic orientation of the methyl groups (and a reduction in SF intensity), while the gauche defects in the acyl chains relax the symmetry constraints resulting in an increase in methylene symmetric stretch intensity. Thus, for an all-trans chain, the intensity ratio $\sqrt{CH_3SS}/\sqrt{CH_2SS}$ approaches infinity when the methyl symmetric stretch is strong and the methylene symmetric stretch is absent, while a much smaller ratio is expected for highly disordered chains as the methylene mode becomes dominant over the methyl mode. Although the methyl symmetric stretch intensity is split by Fermi resonance to yield the intensity in the two peaks at 2880 and 2940 cm$^{-1}$, we will include only the one at 2880 cm$^{-1}$ in the ordering parameter for the following four reasons. First, the degree of mixing between the two states should not be dependent on methyl group orientation based on symmetry considerations. Second, experimentally the splitting between the peaks does not change with orientation whereas the splitting is very sensitive to the mixing of the states. Third, the $CH_3SS$ and $CH_3FR$ intensities track together as a function of chain length and order. Finally, this is the parameter that has been utilized in the literature and is maintained here for consistency.

The intensity ratios are presented in Table 2 for each of the monolayers studied at the vapor/$D_2O$ interface. Recall that the ordering parameter utilizes the peaks at approximately 2850 and 2880 cm$^{-1}$ that appear in most of the spectra as a large peak with a small shoulder on the low energy side. The change in

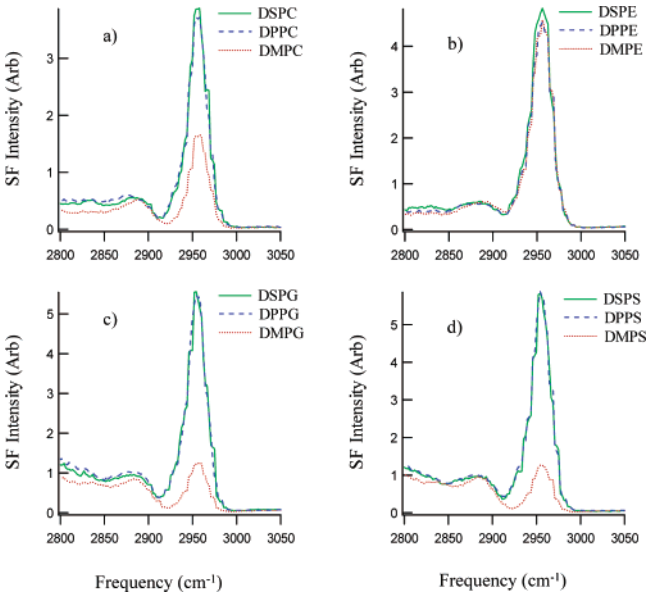


**Figure 3.** Sum-frequency spectra of phospholipid monolayers in the C−H stretching region at the vapor/$D_2O$ interface (10 mM phosphate buffer pD 7.0) acquired under *sps* polarization. (a) Phosphatidylcholines, (b) phosphatidylethanolamines, (c) phosphatidylglycerols, (d) phosphatidylserines.

order for the phosphatidylcholines from 2.5 for DMPC to 7.9 for DSPC mirrors what has been found in a previous study on cholines at the $CCl_4/D_2O$ interface: relative disorder for $C_{14}$ chains and relatively strong order for $C_{18}$ chains.[23] The ethanolamines are relatively ordered for all three chain lengths with DMPE exhibiting slightly less order than the others. The onset of order at shorter chain lengths for the ethanolamines compared to the cholines is consistent with the smaller headgroup of the ethanolamines that allows the acyl chains to get closer together, resulting in increased van der Waals interactions. The chain order parameters indicate that DSPE is less ordered than DPPE, but the difference in the order parameter can be attributed to the larger experimental uncertainties in fitting the smaller $CH_2SS$ peak as the chain order increases. The glycerols and serines show a large degree of disorder for the $C_{14}$ chains, with the $C_{16}$ and $C_{18}$ chains more ordered and equally ordered. These two groups of phospholipids have charged headgroups that would be expected to repel each other, leading to decreased chain−chain interactions. However, recent molecular dynamics[34] and IR[35] studies suggest that DPPG headgroups can form hydrogen bonds with neighboring headgroups, which draws the headgroups together, facilitating chain interactions. Recent molecular dynamics studies[1] suggest that DPPS headgroups can hydrogen bond with each other in a fashion similar to ethanolamine headgroups. Overall, the results for all four headgroups show that chain ordering increases with increasing chain length, and that the degree of chain order is the same for $C_{16}$ and $C_{18}$ chains for all four headgroups.

In the *sps* spectra of monolayers of phosphatidylcholine, phosphatidylethanolamine, phosphatidylglycerol, and phosphatidylserine shown in Figures 3a−d, respectively, the $CH_3AS$ is the main feature at ~2960 $cm^{-1}$ (Table 1) with a contribution from $CH_2AS$ between 2897 and 2910 $cm^{-1}$. Included in the fit of each spectrum are a nonresonant contribution and a tail from the O−D stretch band, as there is a significant overlap of the C−H and O−D intensity in *sps* for charged monolayers. There is a larger uncertainty in the position of the $CH_2AS$ than in the other peaks in the *ssp* and *sps* spectra due to the low intensity of this mode and the O−D overlap, making this region of the *sps* spectrum difficult to fit. The intensity of the $CH_3AS$ as a function of chain length agrees well with the results for the $CH_3SS$ in the *ssp* spectra, supporting the conclusion that the methyl groups orient more strongly along the surface normal as the acyl chain length is increased. The absence of $CH_3SS$ intensity in the *sps* spectrum along with the absence of $CH_3AS$ intensity in the *ssp* spectrum suggests that the methyl groups are oriented isotropically about the surface normal.

**Water Structure.** Previous work in this laboratory using isotopic dilution studies has shown that the hydrogen bonding interactions at the neat vapor/water interface are liquidlike with the major contributions to the *ssp* VSFS spectrum arising from the stretching of uncoupled donor O−H oscillators and tetrahedrally coordinated molecules in environments more characteristic of bulk liquid water than of bulk ice.[20,36] There is a strong narrow peak at ~3700 $cm^{-1}$ from free O−H oscillators with the corresponding donor O−H oscillators appearing at 3420 $cm^{-1}$. There are also contributions at 3310 $cm^{-1}$ and to a lesser extent at 3200 $cm^{-1}$ from tetrahedrally coordinated water molecules with the peak at 3310 $cm^{-1}$ comparable in intensity to that at 3420 $cm^{-1}$. These features along with the C−H stretch peaks determined from the vapor $D_2O$ spectra were used in fitting the vapor/$H_2O$ spectra.

When the same phospholipid monolayers as those described above are examined at the vapor/$H_2O$ interface and the O−H stretching spectrum is measured, it was found that chain length had no discernible effect on the water spectrum. Therefore, only the dimyristoyl lipids ($C_{14}$) will be explicitly discussed with the understanding that the discussion also applies to the other chain lengths as well. Additionally, due to the presence of the monolayers, the free O−H oscillators are no longer present at the interface and are consequently not included in the spectral analysis.

The top of Figure 4 shows *ssp* spectra for each lipid at the vapor/$H_2O$ interface at pH 7.0 (10 mM phosphate buffer). The peaks in the C−H region are disproportionately large for DMPE because the order in this monolayer is much greater than in the other layers as described above. In addition to changing the distribution of intensity in the water region relative to the neat interface, each phospholipid headgroup also enhances the observed intensity relative to the neat vapor/$H_2O$ spectrum. Two factors contribute to this enhanced intensity: increased alignment of water molecules perpendicular to the interface and an increase in the sampling depth. In second harmonic studies of charged interfaces[37,38] and VSF studies of charged surfactants at liquid surfaces,[39] enhancement in the water signal has been attributed to alignment of water molecules by the electric field at the interface and to a contribution from a third-order nonlinear susceptibility that arises from the combination of the static field with the laser fields.

DMPC and DMPE show a smaller enhancement in the water spectrum relative to DMPG and DMPS. Although DMPC and DMPE are not charged species, they are zwitterionic, and the charge separation in the headgroup gives rise to a smaller net electric field. From the fits, the greatest intensity for these two phospholipid monolayers is in the 3200 $cm^{-1}$ region indicating significant tetrahedral coordination between water molecules near the interface. We attribute the small but significant differences between the DMPC and DMPE spectra at 3200 and 3600 $cm^{-1}$ to the differences in hydrogen bonding between the headgroup and surrounding water molecules. DMPE can hydrogen bond with water molecules through the amine and through the phosphate moieties, whereas the cholines can hydrogen bond through the phosphate.[11] Greater hydrogen

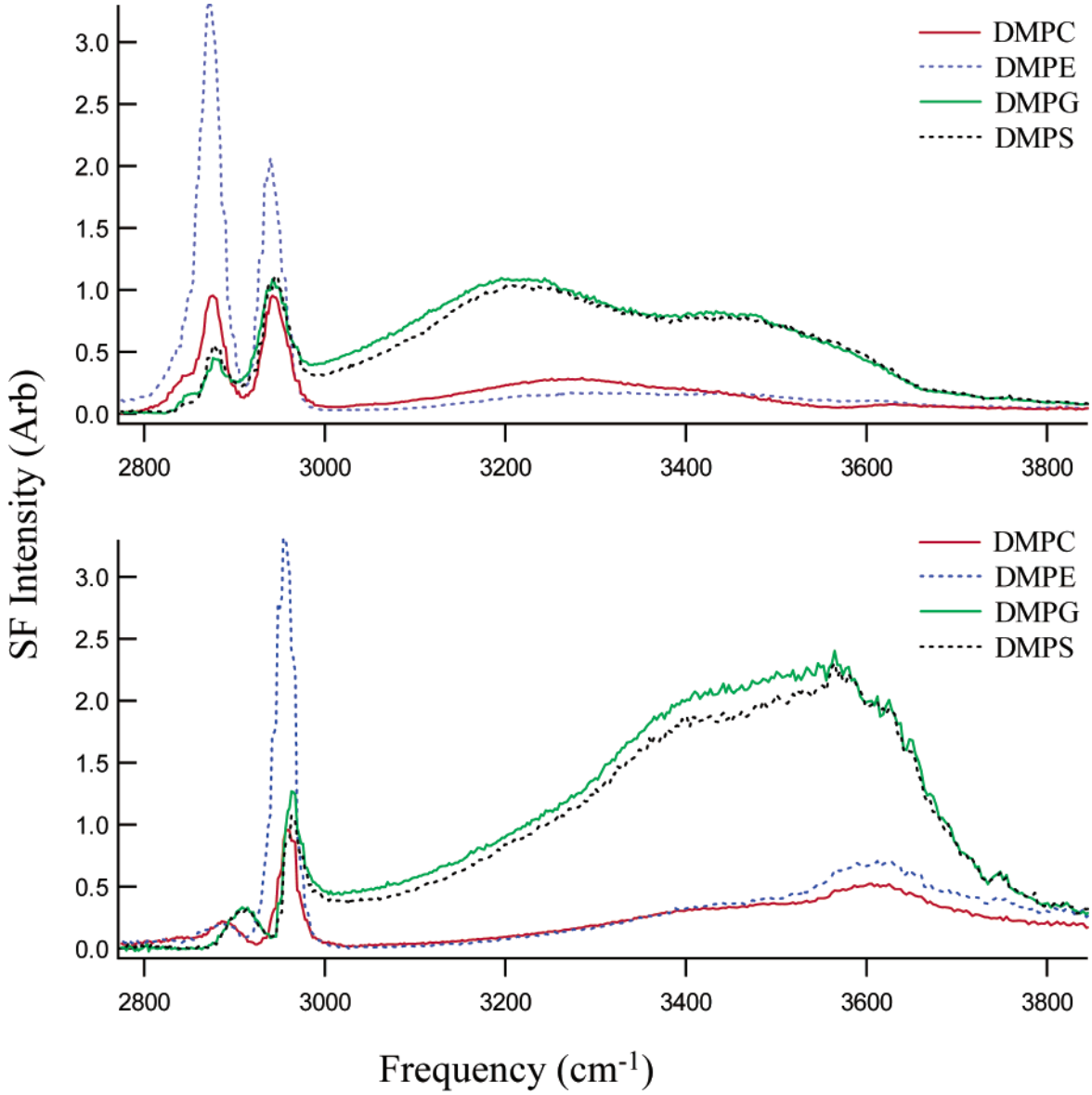


**Figure 4.** Sum-frequency spectra of phospholipid monolayers with $C_{14}$ chains in the C−H and O−H stretching regions at the vapor/$H_2O$ interface (10 mM phosphate buffer pH 7.0) acquired under *ssp* polarization (top) and *sps* polarization (bottom).

bonding between the headgroups and the adjacent water molecules would lead to more disorder in the hydrogen bonding network of water around the headgroup, resulting in less intensity from highly coordinated water molecules and more intensity from less coordinated water molecules, consistent with the results of the spectral analysis.

DMPG and DMPS each carry a negative charge at this pH, resulting in an electric field and electric double layer at the interface. As a result a significant enhancement in the water signal is observed here that is similar to that observed for other charged surfactants at vapor/liquid and liquid/liquid surfaces.[39,40] The spectra of these two lipid monolayers are very similar in the water region, indicating that either the water solvating the headgroups have similar bonding character, or, more likely, that the VSFS signal is dominated by water in the interfacial region as defined dimensionally by the depth of the electric double layer which should be similar for the two monolayers. Similar to the choline, there is a large contribution from tetrahedrally coordinated water molecules in the interfacial region. There is also an increase in intensity from the other peaks associated with varying degrees of hydrogen bond coordination (3200, 3310, and 3420 $cm^{-1}$) that have been found at the vapor/water interface.

The bottom of Figure 4 shows *sps* spectra from monolayers containing each of the four headgroups. There is very little intensity in the neat vapor/$H_2O$ spectrum for this polarization. Each spectrum shows significant intensity above 3400 $cm^{-1}$, indicative of water molecules participating in weak hydrogen bonding interactions similar to those observed in Raman and IR studies of solvating water molecules in aqueous salt solutions.[41−45] We attribute the intensity in this region to water molecules participating in hydrogen bonding with the headgroup. Again, the choline and ethanolamine exhibit similar spectra. We attribute the small but significant difference in intensity at 3600 $cm^{-1}$ to differences in hydrogen bonding between the headgroups and water, consistent with the interpretation of the *ssp* spectra. The peak for solvating water molecules as determined from the *sps* spectra was incorporated into the fits of data from both polarization combinations in order to get consistent phase relationships and peak positions for all the spectra, although water molecules are preferentially aligned to a significant depth

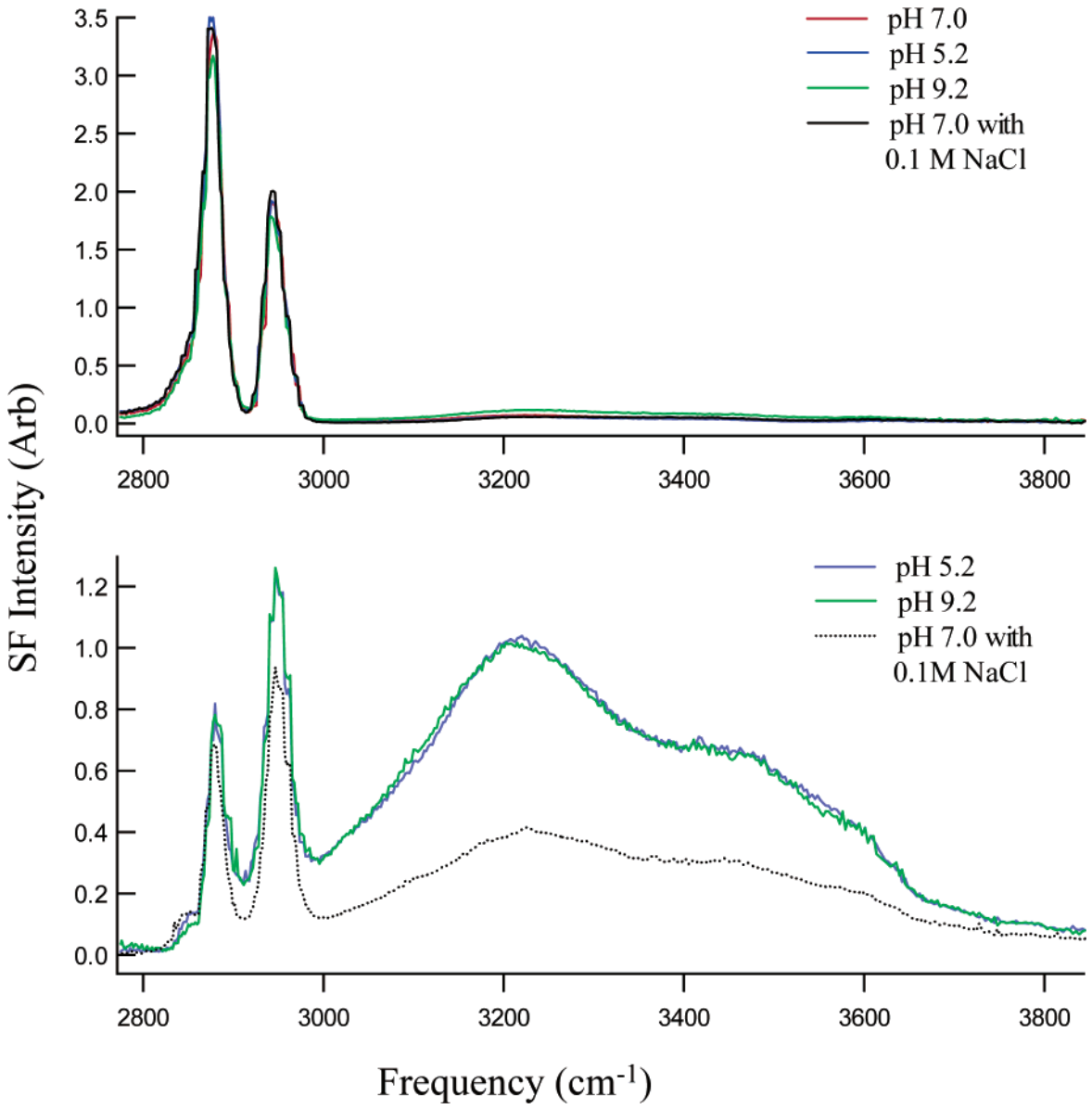


**Figure 5.** Sum-frequency spectra under *ssp* polarization of (a) DMPE monolayers at the vapor/$D_2O$ interface with 10 mM phosphate buffer at pH 5.3, 7.0, 9.3, and pH 7.0 with 0.1 M NaCl, (b) DMPS monolayers at the vapor/$D_2O$ interface with 10 mM phosphate buffer at pH 5.3, 9.3, and pH 7.0 with 0.1 M NaCl.

along the surface normal due to the electric field, and the in-plane orientation of water molecules should become isotropic much closer to the interface. The negatively charged lipids again show a significant enhancement in the water signal, but in the region of weak hydrogen bonding interactions including headgroup solvating water molecules. As above, some of this intensity may be attributed to the lifting of symmetry constraints due to third-order processes involving the DC field.

Since proper pH and electrolyte levels are important to successful biological function, the effects of small changes in pH and the presence of electrolyte on the water structure of these monolayer systems was examined. The top of Figure 5 shows *ssp* spectra of DMPE at pH 5.25, 7.00, and 9.27 and pH 7.00 with 0.1 M NaCl. These spectra and the same ones for DMPC (not shown) indicate that a pH range covering ~4 orders of magnitude in hydrogen ion concentration, does not affect the water structure and that the salt has little to no effect on the alignment of water molecules in the presence of the phospholipids. Similarly, pH in the same range does not affect the water structure associated with the charged monolayers of DMPG (not shown) and DMPS (Figure 5 bottom). However, the addition of salt does have a large effect on the intensity in the water region. The structuring of the water appears to be the same, but the intensity has dropped. This decrease in intensity is attributed to the screening of the monolayer charge by the salt which reduces the penetration of the electric field into the aqueous phase (reducing the double layer thickness), resulting in fewer water molecules being probed.

## Conclusions

Vibrational sum-frequency spectroscopy was employed to investigate acyl chain ordering in a series of phospholipid monolayers at the vapor/water interface and the hydrogen bonding interactions of the water molecules associated with the monolayer. Acyl chain ordering increased with increased chain length for three of the phospholipids studied (diacylphosphatidycholines, diacylphosphatidylglycerols, and diacylphosphatidylserines) and remained constant for the diacylphosphatidylethanolamines. The degree of chain order was consistent for all four headgroups for chain lengths of 16 and 18 carbons. The similarities in chain ordering for phospholipids with such

differing headgroups suggests that the chain ordering of a phospholipid monolayer or bilayer is dominated by the length of the acyl chains and that the different headgroups primarily exert their influence on the water structure at the surface of the monolayer or bilayer.

The presence of the phospholipid monolayers causes an increase in orientation and bonding of water molecules in the interfacial region. This is attributed to the electric fields established at the interface by the headgroups. These effects are significant whether the phospholipids are zwitterionic or they carry a net charge. The spectra that probe changing dipoles perpendicular to the interface show intensity indicative of hydrogen bonding between water molecules; however, spectra that probe changing dipoles in the plane of the interface show the most intensity at frequencies similar to those observed for water molecules solvating complex salts ($\sim$3600 $cm^{-1}$). This intensity is attributed to water molecules solvating the phospholipid headgroups.

Changes in pH from 5.2 to 9.2 have no effect on the orientation and hydrogen bonding of water molecules associated with the monolayer for each lipid headgroup studied. Excess salt has a large effect on the orientation of water molecules and the depth to which water molecules associated with the charged lipids (phosphatidylglycerol and phosphatidylserine) are probed due to the reduction of the double layer thickness. However, it has a negligible effect on the orientation and hydrogen bonding of water molecules associated with the monolayers of the zwitterionic lipids (phosphatidylcholine and phosphatidylethanolamine) which have a much smaller double layer.

These studies suggest that although phosphatidylcholine is the most common and most studied phospholipid, the other phospholipids studied here form monolayers that are as well ordered as the phosphatidylcholine. Subsequently, the study of the interactions between the various phospholipids and large biomolecules, including peptides and proteins, will aid in elucidating their function in biological membranes.

**Acknowledgment.** The authors are grateful for the financial support provided by the National Science Foundation, CHE 9725751, and by the Office of Naval Research for instrumentation.

## References and Notes

(1) Pandit, S. A.; Berkowitz, M. L. *Biophys. J.* **2002**, *82*, 1818−1827.
(2) Denisov, G.; Wanaski, S.; Luan, P.; Glaser, M.; McLaughlin, M. *Biophys. J.* **1998**, *74*, 731−744.
(3) Huang, J.; Swanson, J. E.; Dibble, A. R. G.; Hinderliter, A. K.; Feigenson, G. W. *Biophys. J.* **1993**, *64*, 413−425.
(4) Phillips, M. C. *Prog. Surf. Membr. Sci.* **1972**, *5*, 139−221.
(5) Jones, M. N.; Chapman, D. *Micelles, Monolayers and Biomembranes*; Wiley-Liss: New York, 1994.
(6) Cevk, G.; Marsh, D. *Phospholipid Bilayers*; John Wiley and Sons: New York, 1987; Vol. 5.
(7) Phillips, M. C.; Chapman, D. *Biochim. Biophys. Acta* **1968**, *163*, 301−313.
(8) Caffrey, M. *LIPIDAT: A database of thermodynamic data and associated information on lipid mesomorphic and polymorphic transitions*; CRC Press: Boca Raton, FL, 1993.
(9) Caffrey, M.; Hogan, J. *Chem. Phys. Lipids* **1992**, *61*, 1−109.
(10) Robertson, B.; van Golde, L. M. G.; Batenburg, J. J. *Pulmonary Surfactant*; Elsevier: Amsterdam, 1992; p 753.
(11) Yeagle, P. *The structure of biological membranes*; CRC Press: Boca Ratan, FL, 1991; p 1227.
(12) Bloembergen, N.; Pershan, P. S. *Phy. Rev.* **1962**, *128*, 606−622.
(13) Zhu, X. D.; Suhr, H.; Shen, Y. R. *Phys. Rev. B* **1987**, *35*, 3047−3050.
(14) Guyot-Sionnest, P.; Hunt, J. H.; Shen, Y. R. *Phys. Rev. Lett.* **1987**, *59*, 1597−1600.
(15) Miranda, P. B.; Shen, Y. R. *J. Phys. Chem. B* **1999**, *103*, 3292−3307.
(16) Bain, C. D.; Davies, P. B.; Ong, T. H.; Ward, R. N.; Brown, M. A. *Langmuir* **1991**, *7*, 1563−1566.
(17) Dick, B.; Gierulsky, A.; Marowsky, G. *Appl. Phys. B* **1985**, *38*, 107−116.
(18) Shen, Y. R. *The Principles of Nonlinear Optics*; Wiley: New York, 1984.
(19) Lobau, J.; Wolfrum, K. *J. Opt. Soc. Am. B* **1997**, *14*, 2505−2512.
(20) Raymond, E. A.; Tarbuck, T. L.; Richmond, G. L. *J. Phys. Chem. B* **2002**, *106*, 2817−2820.
(21) Allen, H. C.; Raymond, E. A.; Richmond, G. L. *J. Phys. Chem. A* **2001**, *105*, 1649−1655.
(22) Gragson, D. E.; McCarty, B. M.; Richmond, G. L.; Alavi, D. S. *J. Opt. Soc. B* **1996**, *13*, 2075−2083.
(23) Smiley, B.; Richmond, G. L. *J. Phys. Chem. B* **1999**, *103*, 653−659.
(24) Snyder, R. G.; Strauss, H. L.; Elliger, C. A. *J. Phys. Chem.* **1982**, *86*, 5145−5150.
(25) MacPhail, R. A.; Strauss, H. L.; Snyder, R. G.; Elliger, C. A. *J. Phys. Chem.* **1984**, *88*, 334−341.
(26) Ward, R. N.; Duffy, D. C.; Davies, P. B.; Bain, C. N. *J. Phys. Chem.* **1994**, *98*, 8536−8542.
(27) Walker, R. A.; Gruetzmacher, J. A.; Richmond, G. L. *J. Am. Chem. Soc.* **1998**, *120*, 6991−7003.
(28) Walker, R. A.; Conboy, J. C.; Richmond, G. L. *Langmuir* **1997**, *13*, 3070−3073.
(29) Goates, S. R.; Schofield, D. A.; Bain, C. D. *Langmuir* **1999**, *15*, 1400−1409.
(30) Liu, Y.; Wolf, L. K.; Messmer, M. C. *Langmuir* **2001**, *17*, 4329−4335.
(31) Wolfrum, K.; Laubereau, A. *Chem. Phys. Lett.* **1994**, *228*, 83−88.
(32) Hirose, C.; Akamatsu, N.; Domen, K. *Appl. Spectrosc.* **1992**, *46*, 1051−1072.
(33) Hirose, C.; Akamatus, N.; Domen, K. *J. Chem. Phys.* **1992**, *96*, 997−1004.
(34) Kaznessis, Y. N.; Kim, S.; Larson, R. G. *Biophys. J.* **2002**, *82*, 1731−1742.
(35) Dicko, A.; Bourke, H.; Pezolet, M. *Chem. Phys. Lipids* **1998**, *96*, 125−139.
(36) Raymond, E. A.; Tarbuck, T. L.; Brown, M. G.; Richmond, G. L. *J. Phys. Chem. B*, submitted.
(37) Zhao, X.; Ong, S.; Eisenthal, K. B. *Chem. Phys. Lett.* **1993**, *202*, 513−520.
(38) Ong, S.; Zhao, X.; Eisenthal, K. B. *Chem. Phys. Lett.* **1992**, *191*, 327−335.
(39) Gragson, D. E.; Richmond, G. L. *J. Am. Chem. Soc.* **1998**, *120*, 366−375.
(40) Gragson, D. E.; McCarty, B. M.; Richmond, G. L. *J. Am. Chem. Soc.* **1997**, *119*, 6144−6152.
(41) Strauss, I. M.; Symons, M. C. R. *J. Chem. Soc., Faraday Trans.* **1978**, *1*, 2518−2529.
(42) Walrafen, G. E. *J. Chem. Phys.* **1971**, *55*, 768−792.
(43) Wall, T. T.; Hornig, D. F. *J. Chem. Phys.* **1967**, *47*, 784−792.
(44) Schultz, J. W.; Hornig, D. F. *J. Phys. Chem.* **1961**, *65*, 2131−2138.
(45) Walrafen, G. E. *J. Chem. Phys.* **1970**, *52*, 4176−4198.